Rayleigh-Taylor instability in elastic solids

A. R. Piriz, J. J. López Cela, and O. D. Cortázar
E.T.S.I. Industriales, Universidad de Castilla–La Mancha, 13071 Ciudad Real, Spain

N. A. Tahir
Gesellschaft für Schwerionenforschung Darmstadt, Planckstrasse 1, 64291 Darmstadt, Germany

D. H. H. Hoffmann
Institut für Kernphysik, Technische Universität Darmstadt, 64289 Darmstadt and Gesellschaft für Schwerionenforschung Darmstadt, Planckstrasse 1, 64291 Darmstadt, Germany

(Received 15 June 2005; revised manuscript received 6 September 2005; published 9 November 2005)

We present an analytical model for the Rayleigh-Taylor instability that allows for an approximate but still very accurate and appealing description of the instability physics in the linear regime. The model is based on the second law of Newton and it has been developed with the aim of dealing with the instability of accelerated elastic solids. It yields the asymptotic instability growth rate but also describes the initial transient phase determined by the initial conditions. We have applied the model to solid/solid and solid/fluid interfaces with arbitrary Atwood numbers. The results are in excellent agreement with previous models that yield exact solutions but which are of more limited validity. Our model allows for including more complex physics. In particular, the present approach is expected to lead to a more general theory of the instability that would allow for describing the transition to the plastic regime.

DOI: 10.1103/PhysRevE.72.056313 PACS number(s): 47.20.−k, 52.58.Hm, 52.50.Lp

I. INTRODUCTION

The high intensity heavy ion beam that will be delivered by the future FAIR (Facility for Antiproton and Ion Research) facility [1] to be constructed at Gesellschaft für Schwerionenforschung (GSI) Darmstadt will be a very efficient tool for the creation of high energy density states of matter in the laboratory. One of the experimental schemes proposed for the study of the thermophysical (especially equations of state) and transport properties of high energy density matter in the framework of the FAIR project is the LAPLAS (Laboratory of Planetary Sciences) experiment [2]. This experiment involves a low entropy implosion of a test material, like frozen hydrogen, in order to achieve a high degree of compression while keeping the temperature of the sample relatively low. A typical experiment considers a cylindrical target consisting of the sample material surrounded by a thick shell of heavy material, typically gold or lead (Fig. 1). One face of the target is irradiated with an intense heavy ion beam that has an annular (ring-shaped) focal spot. The inner radius of the annulus is larger than the radius of the sample material in order to avoid direct heating of the sample by the ion beam. Moreover, the outer radius of the focal spot is smaller than the outer radius of the surrounding shell. Thus, when the annular region is heated by the ion beam, it expands, thereby pushing the inner layers of the target (the pusher) and compressing the material sample in the axial region. The external layer around the beam-heated zone remains as a tamper that confines the implosion for a longer time.

This target configuration has recently been studied by means of numerical simulations and analytical models [3–8]. We have shown that such a configuration is very suitable for an experiment dedicated to the study of the hydrogen metallization problem [9,10]. Nevertheless, a challenging problem in this target design is generation of an annular focal spot. A possible system to produce such an annular spot considers a high frequency rf wobbler that will rotate the ion beam with a frequency of the order of gigahertz [11]. We have recently analyzed the symmetry constraints imposed by the wobbler and we have found that a level of symmetry of 1% in the driving pressure can be achieved provided that the beam performs about ten revolutions during the pulse duration [12,13]. This value is equal to the expected intrinsic symmetry level of the system and hence a larger number of revolutions cannot improve the implosion symmetry any further.

Although the rotating beam can provide an acceptable level of symmetry, the stability of the pusher during the implosion still remains another issue of possible concern. In fact, the Rayleigh-Taylor (RT) instability will arise at the pusher/absorber interface during the acceleration phase and later at the pusher/hydrogen interface during the stagnation

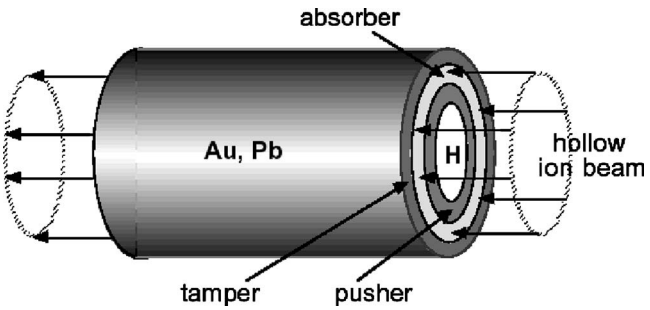

FIG. 1. LAPLAS (Laboratory of Planetary Sciences) experimental scheme. Multilayer target irradiated by a hollow ion beam. The internal sample (H) is surrounded by successive layers constituting the pusher, the absorber, and the tamper.

phase. As it is well known, the RT instability occurs when a higher density fluid lies above a lower density fluid or, equivalently, when the low density fluid pushes and accelerates the heavier one. Under the conditions of the LAPLAS experiment the pusher will be accelerated by a driving pressure of few megabars achieving accelerations of the order of $10^{13}\ \mathrm{cm/s^2}$. During the implosion the pusher remains mainly solid although its internal layers are melted during the deceleration phase, so that it retains the elastic and plastic properties of the material during most of the implosion process. On the other hand, the absorber region is melted during the phase of heating and then it remains in a liquid state the rest of the implosion time. Up to a certain extent the situation is similar to that present in magnetically accelerated shells [14–16] and in shells accelerated by gaseous detonation products [17–20]. A brief review of the experimental and theoretical work on the RT instability in solids has been recently published in Ref. [21].

The physics of the RT instability in solids is significantly determined by such elastoplastic properties of the material and it shows a series of complex phenomena that are not well understood yet. In this regard, the analysis of situations involving materials with pure elastic or plastic properties may be of great help as a previous step in the construction of a more complete theory describing the transition from elastic to plastic regimes.

The problem of the linear RT instability in perfectly elastic solids has previously been studied by different methods. The so-called one-degree-of-freedom models give a qualitative description of the instability but they considerably underestimate the growth rate [22–24]. Similar results have also been found by different theoretical methods in Ref. [25]. Besides, an exact solution has been given in Ref. [26], where an implicit formula for the growth rate has been obtained. The last work, like all the previous ones, is limited to the situation in which the instability developed on a solid/vacuum interface (or solid/ideal gas), so that the Atwood number A_T is equal to 1 $[A_T=(\rho_{solid}-\rho_{gas})/(\rho_{solid}+\rho_{gas})]$. Recently Terrones [21] has obtained an exact solution for arbitrary Atwood numbers that applies to solid/solid and solid/viscous fluids interfaces. This model is based on a normal mode linear analysis, so that it yields a growth rate that coincides with the results of Ref. [26] (for $A_T=1$) once the asymptotic regime has been reached. That is, it cannot describe the initial transient phase determined by the initial conditions. The knowledge of this initial phase is essential in order to determine the later evolution of the perturbation amplitude. Although the works presented in Refs. [21,26] are somewhat limited because the latter is restricted to Atwood number $A_T=1$ and the former describes only the asymptotic regime (and therefore loses the information about the initial conditions), they are of great relevance as they are the only exact results available for the problem of the linear RT instability in elastic solids. Thus, they allow for testing more general, albeit approximate, theories. Such approximate theories seem to be necessary to deal with more complex problems for which the previous models are not suitable. In fact, they are sufficiently involved mathematically to make it difficult to include some important physical aspects present in realistic situations; namely, the effect of density gradients, finite thickness of the accelerated layer, the existence of an initial phase in which the driving pressure rises from zero to its maximum value, and others. In particular, those models seem to be inadequate for studying the transition from elastic to plastic regime.

The relatively simple one-degree-of-freedom models based on an energy balance equation [22–24] can certainly deal with more realistic physics but they are not sufficiently accurate to account for the results observed in the simulations [29] and they do not agree with the exact solutions of Refs. [21,26].

In this paper we present a model that can also be considered as a sort of one-degree-of-freedom model but that is based on the second law of Newton instead of on an energy balance. It produces explicit analytical results in excellent agreement with the models of Refs. [21,26] and allows for including more of the physical effects present in realistic situations. The model also describes the transient phase between the initial conditions and the asymptotic regime and shows how the perturbation growth in the asymptotic regime depends on the initial conditions. In particular, for $A_T=1$, it is in excellent agreement with Ref. [26] and, for arbitrary Atwood numbers, it yields an asymptotic growth rate for solid/solid and for solid/fluid interfaces that agree with Ref. [21] within 15%. The possibility of dealing with different initial conditions is of great importance because the RT instability stage can in practice be preceded by a Ritchmyer-Meshkov (RM) unstable phase [27,28], and/or by a ramp in the driving pressure [29] or by any other particular experimental situation which cannot be taken into account in the asymptotic regime calculations.

II. ANALYTICAL MODEL

A. Fundamental equations

Most of the analytical models developed in the past for studying the effect of the solid properties on the RT instability growth rate in an accelerated plate have been based on an energy balance equation [22–24,30]. As far as we are aware, the first attempt to use an energy balance to analyze the RT instability was performed by Fermi in 1955 [31] with the aim of deriving the classical results [32] for inviscid incompressible fluids in an intuitively appealing manner. However, these models do not yield, in general, quantitatively correct results [24,29]. An alternative approach consists in using the Newton second law in order to derive the equation of motion of the interface from the balance of forces acting on it. Such an analysis has been used in the past for the study of the instability of an accelerated rigid plastic slab [33]. Actually force and energy balance approaches must be equivalent and they should give the same results provided that they are treated consistently. In fact, the mechanical energy balance is obtained from the momentum conservation equation (the Cauchy equation) by multiplying it by the velocity and then integrating over a volume [29,34,35]. However, models based on the energy balance have inconsistently dealt with the main model assumption, namely, that the field velocities can be approximated by the one corresponding to an inviscid fluid. This approximation is entirely reasonable and we also

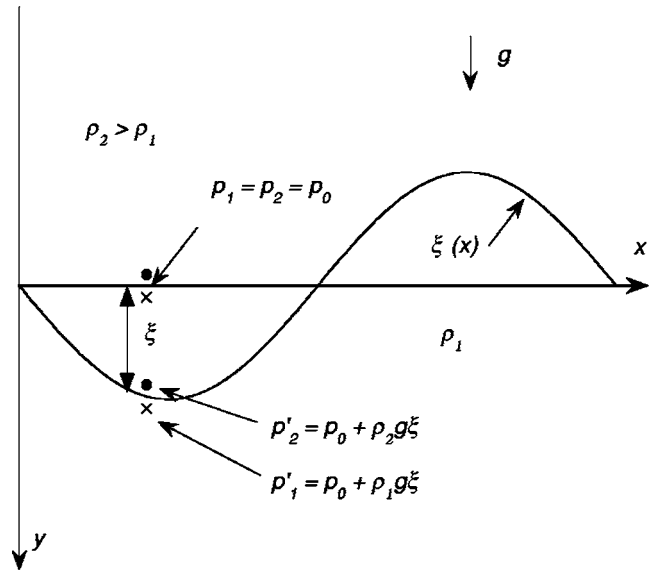

FIG. 2. Diagram of the perturbed interface.

will adopt it here [see Eqs. (14) and (16)]. Nevertheless, by using a solenoidal and irrotational velocity field we run into a version of the Poritsky paradox [36,37] because the term containing the deviatoric part S_{ij} of the stress tensor results to be zero ($\partial S_{ij}/\partial x_j = 0$), so that, apparently, no difference exists between the equations governing the instability of an inviscid fluid and those for a nonideal fluid. Actually, the nonideal effects manifest themselves through the boundary condition on the interface and not through the Cauchy equations, thus resolving the paradox [36,37]. These considerations were overlooked in the past when dealing with the energy balance equation and, as a consequence, only results of qualitative character were obtained. The analysis based on the force balance is more intuitive and allows for introducing the boundary condition on the interface conveniently.

Let us briefly show how the classical result results from the force balance approach. We consider two inviscid fluids so that the denser fluid of density ρ_2 lies above the lighter fluid of density ρ_1 where $\rho_1 < \rho_2$ (Fig. 2). If the interface is perfectly planar and it is in equilibrium, the fluid elements on each side of the interface immediately above and below it, respectively, have the same pressure $p_1 = p_2 = p_0$. If we introduce a small perturbation $\xi(x)$ in the surface, so that these fluid elements originally at $y=0$ are (quasistatically) translated to a lower position $y=\xi(x)$, the pressure of the fluid elements will increase as they are in a deeper place within the fluid. However, pressure in the denser fluid increases more than pressure in the lighter one:

$$p_1' = p_0 + \rho_1 g\xi, \quad p_2' = p_0 + \rho_2 g\xi. \tag{1}$$

Therefore, a pressure difference $\Delta p = (\rho_2 - \rho_1) g\xi$ is created which tends to further deform the interface. According to the Newton second law, the equation of motion of the interface can be written as follows:

$$m\ddot{\xi} = \Delta p A, \tag{2}$$

where A is the area of the interface and m is the mass of both fluids involved in the motion. Since in the RT instability we have to deal with surface modes that decay from the interface as $\exp(-ky)$ ($k = 2\pi/\lambda$ is the perturbation wave number and λ is the perturbation wavelength), we can assume that in the linear regime only the fluid within a distance equal to k^{-1} participates in the motion [21–26,29,30,38,39]. Therefore, we get

$$m = m_1 + m_2 = \rho_1 \frac{A}{k} + \rho_2 \frac{A}{k}, \tag{3}$$

where m_1 and m_2 are, respectively, the masses of the light and heavy fluids participating in the motion. Thus the equation of motion reads

$$\frac{(\rho_2 + \rho_1)}{k}\ddot{\xi} = (\rho_2 - \rho_1) g\xi \quad \text{or} \quad \ddot{\xi} = A_T k g \xi, \quad A_T = \frac{\rho_2 - \rho_1}{\rho_2 + \rho_1}. \tag{4}$$

As it is well known, this equation can be easily integrated to get the classical asymptotically exponential amplitude growth with a rate $\gamma = \sqrt{A_T k g}$ [32].

This very simple model clearly shows how the interface motion is driven by the force $(\rho_2 - \rho_1) g\xi A$. If other forces F_i are present, for example due to viscosity, surface tension, elasticity, or plasticity, they should be added to the equation of motion:

$$\frac{d}{dt}[(m_1 + m_2)\dot{\xi}] = (\rho_2 - \rho_1) g\xi A + \sum F_i. \tag{5}$$

So provided that we can calculate the corresponding forces F_i, this equation will describe the evolution of the interface. Let us consider a few examples.

1. Surface tension

The force F_{st} due to surface tension on the interface of two inviscid incompressible fluids can be obtained from the Laplace formula

$$F_{st} = A\Delta p_{st} = A\frac{\sigma_{st}}{R_c}, \tag{6}$$

where σ_{st} is the surface tension coefficient and R_c is the curvature radius of the interface surface $\xi(x)$. The interface curvature radius can be easily obtained from elemental calculus

$$R_c = \frac{[1 + (d\xi/dx)^2]^{3/2}}{d^2\xi/dx^2}. \tag{7}$$

For a sinusoidal perturbation, $\xi(x) \propto \exp(ikx)$ and then we get $R_c \approx -1/k^2\xi$ (for $k\xi \ll 1$). Therefore, the equation of motion of the interface is

$$\ddot{\xi} = \left(A_T k g - \frac{\sigma_{st} k^3}{\rho_1 + \rho_2}\right)\xi. \tag{8}$$

This is the exact result given by the normal modes theory [34].

2. Viscous fluids

For incompressible Newtonian fluids the force on the interface must include the effect of the viscosity. The force f_i

per unit of area acting on the interface surface due to the heavy fluid is [35]

$$f_i^{(2)} = p_2' n_i^{(2)} - S_{ij}^{(2)} n_j^{(2)}, \tag{9}$$

where p_2' is the pressure in the heavy fluid given by Eq. (1), i and j denote the coordinate directions ($i,j=x,y,z$), the indices "2" indicate values in the heavy fluid, $n_j^{(2)}$ is the j component of the unit vector $\mathbf{n}^{(2)}$ directed outward along the normal to the interface, and the deviatoric part of the stress tensor $S_{ij}^{(2)}$ is given by the following constitutive relation [35]:

$$S_{ij}^{(2)} = 2\mu_2 D_{ij}^{(2)}, \quad D_{ij}^{(2)} = \frac{1}{2}\left(\frac{\partial v_i^{(2)}}{\partial x_j} + \frac{\partial v_j^{(2)}}{\partial x_i} \right), \tag{10}$$

where $D_{ij}^{(2)}$ is the strain rate tensor, $v_i^{(2)}$ are the corresponding fluid velocities, and μ_2 is the dynamical viscosity coefficient. Considering two-dimensional perturbations ($i=y,j=x$) and ignoring surface tension, we have for the vertical force

$$f_y^{(2)} = p_2' n_y^{(2)} - S_{yy}^{(2)} n_y^{(2)} - S_{yx}^{(2)} n_x^{(2)}. \tag{11}$$

Since $n_x^{(2)} \sim k\xi \ll 1$ ($n_y^{(2)} \approx 1$), the last term is negligible in the linear regime we are considering and the force per unit of area on the interface due to the heavy fluid turns out to be

$$f_y^{(2)} = p_2' - S_{yy}^{(2)}. \tag{12}$$

Thus the contribution of the deviatoric part of the stress tensor to the force on the interface is

$$F_v^{(2)} = -S_{yy}^{(2)} A = -2\mu_2 \frac{\partial v_y^{(2)}}{\partial y} A. \tag{13}$$

Assuming small perturbations of the form

$$v_y^{(2)} \propto e^{ikx+qy} \tag{14}$$

(q is the longitudinal wave number) we get

$$F_v^{(2)} = -2\mu_2 q v_y^{(2)} A \approx -2\mu_2 k \dot{\xi} A, \tag{15}$$

where we have taken [22–25,30,31,42]

$$q \approx k, \quad v_y^{(2)}(y=0) = \dot{\xi}. \tag{16}$$

Therefore, the total force on the interface due to both fluids that must be included in Eq. (5) is

$$F_v \approx -2(\mu_1 + \mu_2) k^2 \dot{\xi} \frac{A}{k}, \tag{17}$$

where μ_1 and μ_2 are, respectively, the viscosities of fluid 1 (the lighter) and fluid 2 (the heavier). Introducing Eq. (17) into Eq. (5) we find the interface equation of motion:

$$\ddot{\xi} = A_T k g \xi - 2\frac{\mu_1 + \mu_2}{\rho_1 + \rho_2} k^2 \dot{\xi}, \tag{18}$$

and the asymptotic growth rate γ [$\xi \propto \exp(\gamma t)$, where t is the time] is

$$\gamma^2 + (\mu_1 + \mu_2)(1 + A_T) k^2 \gamma - A_T k g = 0. \tag{19}$$

This is a well known and very good approximation to the instability growth rate for the case of pure viscosity (within 11%) that was originally proposed by Bellman and Pennington in 1954 [40] and later obtained by Hide [41] using the variational method of Chandrasekhar [34]. More recently, it was also rederived by Mikaelian by using the method of moment equations [42,43]. A similar approximate equation has also been obtained in Ref. [44] by analyzing the distribution of the roots of the exact relation dispersion in the complex plane. Other authors have produced a less accurate approximation by using methods that are more involved mathematically [24,25,45].

III. RT INSTABILITY IN SOLIDS

A. Perfectly elastic solids

We can apply the previous model to a perfectly elastic medium (a Hookean material). In such a case, the constitutive relation reads [46]

$$\frac{\partial S_{ij}}{\partial t} = 2G D_{ij}, \tag{20}$$

where G is the shear modulus of the material and D_{ij} is given by Eq. (10). Considering two-dimensional perturbations and incompressibility, the force on the interface due to each one of the media turns out

$$\frac{\partial F_e^{(n)}}{\partial t} \approx -2G_n k \dot{\xi} A, \tag{21}$$

where, as before, we have taken $q \approx k$ ($n=1$, 2 denotes the medium). Integrating and assuming as in Refs. [24,26] an initially stress-free material, we get

$$F_e^{(n)} \approx -2G_n k(\xi - \xi_0) A, \tag{22}$$

where ξ_0 is the initial value of the perturbation amplitude.

1. Solid/solid and solid/vacuum interfaces

Now we can consider different situations. For a solid/solid interface the total force due to both elastic solids is

$$F_e \approx -2(G_1 + G_2) k^2 (\xi - \xi_0) \frac{A}{k}, \tag{23}$$

and the equation of motion reads

$$\ddot{\xi} = A_T k g \xi - \frac{(G_1 + G_2)}{\rho_2} (1 + A_T) k^2 (\xi - \xi_0). \tag{24}$$

For the particular case of a solid/vacuum interface we take $G_1=0$ and $\rho_1=0$ (for a solid/ideal fluid interface we should take $G_1=0$ and $\rho_1 \neq 0$) and the previous equation reduces to

$$\ddot{\xi} = A_T k g \xi - \frac{2G_2}{\rho_2} k^2 (\xi - \xi_0). \tag{25}$$

This equation is similar to the one obtained originally by Miles [22] except for the factor of 2 in the term corresponding to the elastic force (Miles obtained a factor of 13/4) and

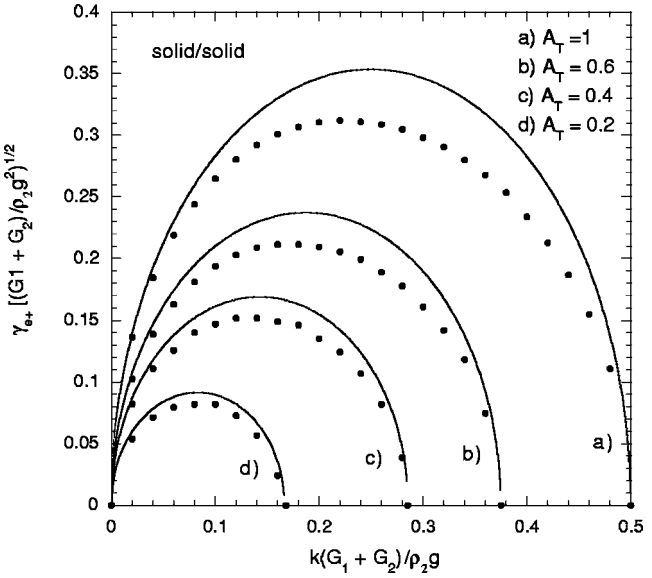

FIG. 3. Asymptotic dimensionless growth rate $\gamma_{e+}[(G_1+G_2)/\rho_2 g^2]^{1/2}$ as a function of the dimensionless perturbation wave number $k(G_1+G_2)/\rho_2 g$ for a solid/solid interface and for several values of the Atwood number A_T. Dots are the exact results of Ref. [21] and full lines are given by the present model.

for the term proportional to ξ_0 coming from the stress-free material initial condition. In Ref. [24] a similar equation has also been obtained but they got a factor of 4 in the elastic force term.

In the asymptotic regime ($t\to\infty$) Eq. (24) gives the following growth rate:

$$\gamma_e = \sqrt{A_T k g - (1+A_T)\frac{(G_1+G_2)}{\rho_2}k^2}, \tag{26}$$

and this equation yields the correct value of the cutoff perturbation wave number beyond which perturbations are stabilized [21]:

$$k_c = \frac{(\rho_2-\rho_1)g}{2(G_1+G_2)}. \tag{27}$$

We have compared the previous expression for the growth rate with the exact results of Ref. [21] in Fig. 3. As can be seen, Eq. (26) reproduces exactly the cutoff wave number. In addition, it gives the value k_m of the perturbation wave number corresponding to the maximum growth rate ($k_m=k_c/2$) in good agreement with the exact value obtained in Ref. [21]. Figure 3 also shows that Eq. (26) gives the values of the growth rate with a practically systematic error of about 15% ($\gamma_e^{exact}\approx 0.85\gamma_e^{model}$). In particular, the maximum growth rate γ_{em} is

$$\gamma_{em} = \frac{A_T}{2\sqrt{1+A_T}}\sqrt{\frac{\rho_2 g^2}{G_1+G_2}}. \tag{28}$$

The asymptotic regime in which the perturbation grows exponentially with a growth rate γ_e is achieved after a transient phase that lasts for a time of the order of γ_e^{-1}. Although this growth rate is independent of the initial conditions, the perturbation amplitude will be affected, in general, by the initial velocity $\dot{\xi}_0$ and acceleration $\ddot{\xi}_0$. These initial conditions are important because the RT phase may start from a surface at rest in a stress-free material or, instead, it may arise after a previous phase dominated by the RM instability [19,27,28], and/or by a transient phase in which the driving pressure increases before reaching a constant value [24,29].

Equation (24) can be integrated to yield the perturbation amplitude as a function of time for both unstable (ξ_+) and stable (ξ_-) cases:

$$\frac{\xi_+}{\xi_0} = 1 + (a_+ + u_+)[\cosh(\gamma_{e+}t) - 1] - u_+(e^{-\gamma_{e+}t} - 1), \tag{29}$$

$$\frac{\xi_-}{\xi_0} = 1 + a_- + \sqrt{a_-^2 + u_-^2}\sin\left[\gamma_{e-}t - \arcsin\left(\frac{1}{\sqrt{1+(u_-/a_-)^2}}\right)\right], \tag{30}$$

where for an initially stress-free solid we have

$$a_\pm = \frac{\ddot{\xi}_0}{\gamma_{e\pm}^2\xi_0} = \pm\frac{1}{1-k/k_c}, \quad \gamma_{e\pm}^2 = \pm A_T k g\left(1-\frac{k}{k_c}\right),$$

$$u_\pm = \frac{\dot{\xi}_0}{\gamma_{e\pm}\xi_0}. \tag{31}$$

For the particular case in which the solid is initially at rest considered in Refs. [26,29], $u_\pm=0$ results and the preceding expressions take the following simple form:

$$\frac{\xi_+}{\xi_0} = 1 + a_+[\cosh(\gamma_{e+}t) - 1], \tag{32}$$

$$\frac{\xi_-}{\xi_0} = 1 + a_-[1 - \cos(\gamma_{e-}t)]. \tag{33}$$

As is seen from Eqs. (31) and (32) in the asymptotic regime ($t\to\infty$) the amplitude of the perturbation is

$$\xi_{+(\infty)}(t) = \frac{\xi_0 a_+}{2}e^{\gamma_{e+}t} = \frac{\xi_0}{2(1-k/k_c)}e^{\gamma_{e+}t}, \tag{34}$$

and the perturbation grows as if initially it would be equal to $\xi_0 a_+/2$, that is, a value dependent on the perturbation wave number and on the physical parameters (Fig. 4). We see that when the perturbation wave number approaches the cutoff value ($k\to k_c$) this effective initial amplitude goes to infinity. This can be clearly appreciated in Fig. 5 where we have compared the value of $\xi_0 a_+/2$ given by our model with the exact results of Ref. [26] for $A_T=1$ and $G_1=0$. It is worth noting that each dot plotted in Fig. 5 has been calculated by using the model of Ref. [26] for different cases varying the parameters k, G_2, ρ_2, and g in order to check the dependence on the dimensionless perturbation wave number k/k_c rather

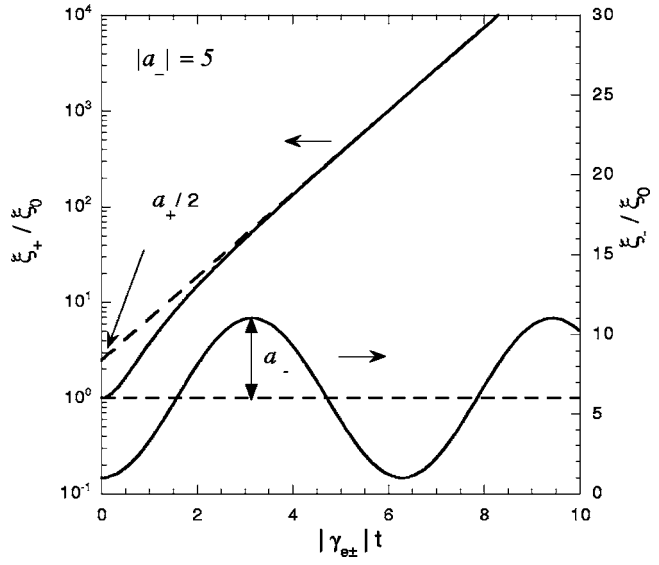

FIG. 4. Dimensionless amplitudes $\xi_\pm/\xi_0$ as a function of the dimensionless time $|\gamma_{e\pm}|t$ for an unstable (+) and a stable (−) case.

than on the individual parameters. In order to make the comparisons we have used Eq. (3.23) of Ref. [26] for the case of very thick layers ($kH \gg 1$, H being the thickness of the solid slab).

Similarly, for the stable cases, when $k > k_c$, Eq. (33) shows that the interface oscillates around the value $(1 + a_-)\xi_0$ with an amplitude $\xi_0 a_- = \xi_0/(k/k_c - 1)$ (Fig. 4). When $k \to k_c$ from the stable side, the oscillation amplitude grows without limit such as was observed in the simulations of Ref. [29]. In Fig. 6 we have compared the dimensionless oscillation amplitude a_- given by our model with the exact results of Ref. [26] ($A_T = 1$, $G_1 = 0$). As in the unstable case, each dot

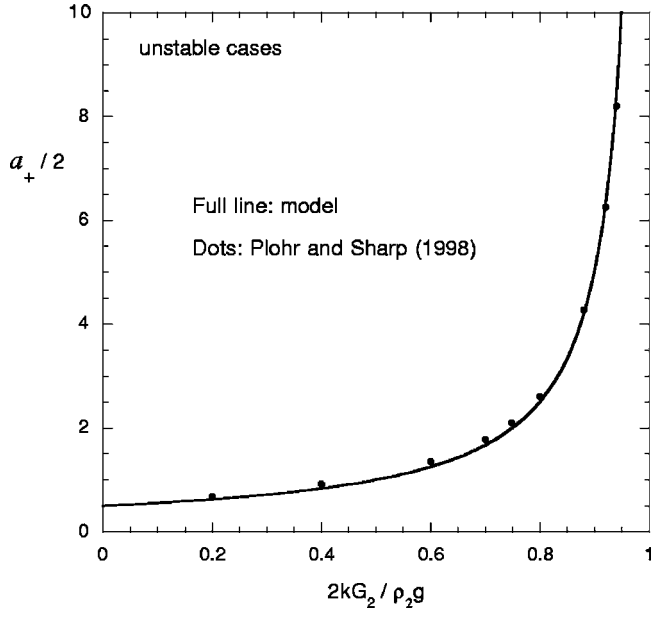

FIG. 5. Asymptotic dimensionless amplitude $a_+/2$ for the unstable cases as a function of the dimensionless perturbation wave number k/k_c, where $k_c = \rho_2 g/2G_2$ is the cutoff perturbation wave number.

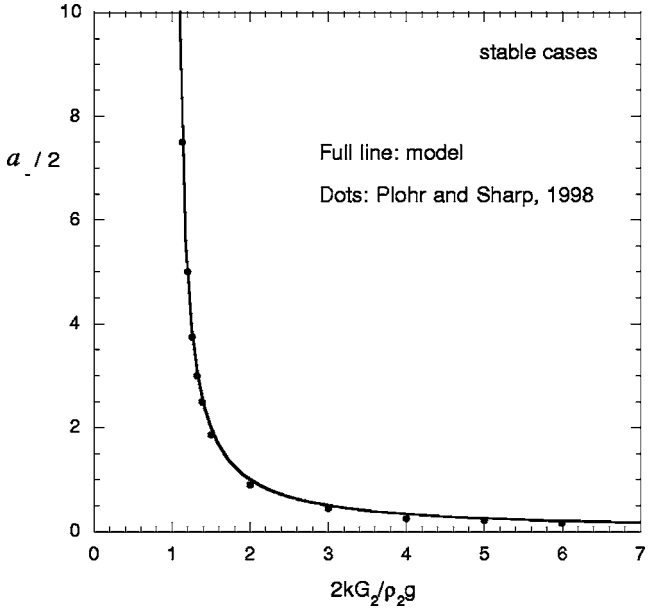

FIG. 6. Asymptotic dimensionless amplitude $a_-/2$ for the stable cases as a function of the dimensionless perturbation wave number k/k_c, where $k_c = \rho_2 g/2G_2$ is the cutoff perturbation wavenumber.

has been obtained for different values of k, G_2, ρ_2, and g producing the same value of k/k_c.

The excellent agreement between the present model and the results of Ref. [26] shown in Figs. 5 and 6 indicates that our model correctly describes the transient phase. In addition, it shows that the instantaneous amplitude cannot be correctly calculated from the results for the asymptotic regime obtained in Ref. [21] because it cannot account for the initial conditions. In order to compare with the results for the case of an initially stress-free solid which is at rest we have taken $a_\pm$ from Eq. (31) and we have also put $u_{0\pm} = 0$, but different initial conditions could be considered in order to take into account the previous history before the RT phase starts or any particular experimental conditions.

2. Solid/viscous fluid interface

In the case in which the lighter medium is a viscous fluid and the heavier one is an elastic solid, such as was considered in Ref. [21], the total force is given by

$$F_{ve} = -2\mu_1 k^2 \dot{\xi}\frac{A}{k} - 2G_2 k^2(\xi - \xi_0)\frac{A}{k}, \tag{35}$$

where we have used Eq. (16) for the viscous fluid and Eq. (22) for an initially stress-free elastic solid. Therefore, the interface equation of motion reads

$$\ddot{\xi} + \frac{\mu_1}{\rho_2}(1 + A_T)k^2\dot{\xi} = A_T k g \xi - \frac{G_2}{\rho_2}(1 + A_T)k^2(\xi - \xi_0), \tag{36}$$

which has explicit solutions for both unstable $[\xi_+(t)]$ and stable $[\xi_-(t)]$ cases. For the particular case of $\dot{\xi}_0 = 0$ it is

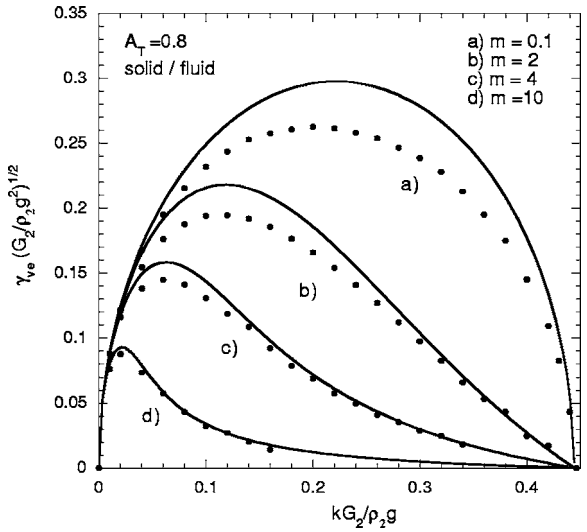

FIG. 7. Asymptotic dimensionless growth rate $\gamma_{ve}(G_2/\rho_2 g^2)^{1/2}$ as a function of the dimensionless perturbation wavenumber $kG_2/\rho_2 g$ for a solid/fluid interface, for an Atwood number $A_T=0.8$ and for several values of the dimensionless viscosity parameter $m=[\mu_1 g(\rho_2/G_2^3)^{1/2}]^{1/2}$. Dots are the exact results of Ref. [21] and full lines are given by the present model.

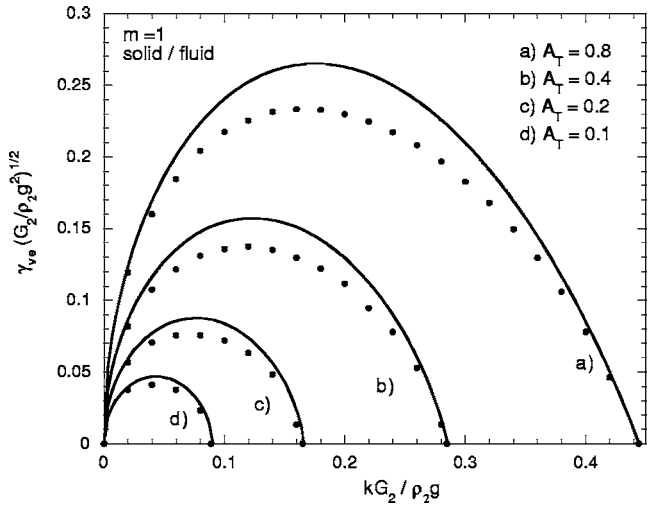

FIG. 8. Asymptotic dimensionless growth rate $\gamma_{ve}(G_2/\rho_2 g^2)^{1/2}$ as a function of the dimensionless perturbation wave number $kG_2/\rho_2 g$ for a solid/fluid interface, for several Atwood numbers A_T and for a dimensionless viscosity parameter $m=[\mu_1 g(\rho_2/G_2^3)^{1/2}]^{1/2}=1$. Dots are the exact results of Ref. [21] and full lines are given by the present model.

$$\frac{\xi_+}{\xi_0} = 1 + a_+\left[e^{-\beta t}\left(\cosh t\sqrt{\gamma_{e+}^2+\beta^2} + \frac{\beta}{\sqrt{\gamma_{e+}^2+\beta^2}}\sinh t\sqrt{\gamma_{e+}^2+\beta^2}\right) - 1\right], \tag{37}$$

$$\frac{\xi_-}{\xi_0} = 1 + a_-\left[1 - e^{-\beta t}\left(\cos t\sqrt{\gamma_{e-}^2-\beta^2} + \frac{\beta}{\sqrt{\gamma_{e-}^2-\beta^2}}\sin t\sqrt{\gamma_{e-}^2-\beta^2}\right)\right], \tag{38}$$

where $a_\pm$ and $\gamma_{e\pm}$ were defined in Eqs. (31) and β is a parameter accounting for the fluid viscosity:

$$\beta = \frac{1+A_T}{2}\frac{\mu_1 k^2}{\rho_2}. \tag{39}$$

Obviously for $\beta=0$ the case of a solid/ideal fluid interface is recovered. For the asymptotic regime, in the unstable case, we get

$$\frac{\xi_{+(\infty)}(t)}{\xi_0} = \frac{a_+}{2}e^{\gamma_{ve}t}, \tag{40}$$

where $\gamma_{ve}=\sqrt{\gamma_{e-}^2+\beta^2}-\beta$ or, using dimensionless parameters and adopting the notation of Ref. [21],

$$\alpha = -\frac{m^2}{2}(1+A_T)\kappa^2 + \sqrt{\left(\frac{m^2}{2}(1+A_T)\kappa^2\right)^2 + A_T\kappa\left(1-\frac{1+A_T}{A_T}\kappa\right)}, \tag{41}$$

where

$$\alpha = \gamma_{ve}\left(\frac{G_2}{\rho_2 g^2}\right)^{1/2}, \quad \kappa = \frac{kG_2}{\rho_2 g}, \quad m^2 = \mu_1 g\left(\frac{\rho_2}{G_2^3}\right)^{1/2}. \tag{42}$$

We can see from Eq. (40) that, as in the case of a solid/solid interface, the perturbation grows as if at $t=0$ it would have had an amplitude equal to $\xi_0 a_+/2$. For the stable cases the oscillation frequency is $\sqrt{\gamma_{e-}^2-\beta^2}$ and the oscillations take place around $(1+a_-)\xi_0$. They start with a value $\xi_0 a_-$ and then they are damped by the term $\exp(-\beta t)$.

The growth rate given by Eq. (41) is compared with the results of Ref. [21] in Fig. 7 for $A_T=0.8$ and several values of the parameter m and in Fig. 8 for $m=1$ and several values of A_T. We can see that, as in the previous case of a solid/solid interface, the wave numbers corresponding to the cutoff and to the maximum growth rate are reproduced exactly. In addition, the growth rate is given with a maximum error of 15% for $m=0$ and it is somewhat less when the effects of viscosity become important.

The previous equations can be easily modified in order to consider more general initial conditions. In particular, for the LAPLAS experiment, we have to deal with a solid/fluid interface that is initially perfectly smooth but that is accelerated by a nonuniform driving pressure. In such a case, $\xi_0=0$, $\dot{\xi}_0=0$, and $\ddot{\xi}_0=(1+A_T)k\Delta p/2\rho_2$, where Δp is the pressure asymmetry and it is of the order of 1% of the driving pressure [13].

B. Rigid plastic solids

It may be instructive to consider here the ideal situation of a perfectly rigid plastic solid in order to get some insight into the RT instability problem when the perturbation amplitude grows beyond the elastic limit. For this we adopt the Levy-

Mises rule for plastic flow with the von Mises yield criterion so that the corresponding constitutive relation reads

$$S_{ij} = \sqrt{\frac{2}{3}} Y \frac{D_{ij}}{|D_{ij}|}, \tag{43}$$

where Y is the yield strength in uniaxial tension. From Eqs. (10) and (14) we have

$$D_{yy} \approx k\dot{\xi}, \quad |D_{\mathrm{ij}}| = \sqrt{2}\, k|\dot{\xi}|. \tag{44}$$

Then, the force per unit of area is obtained:

$$f_p = -S_{yy} = -\sqrt{\frac{1}{3}} Y \frac{\dot{\xi}}{|\dot{\xi}|}, \tag{45}$$

and the resulting equation of motion for the simplest case of a rigid plastic solid/vacuum interface is

$$\ddot{\xi} = kg\xi - \sqrt{\frac{1}{3}} \frac{kY}{\rho_2} \frac{\dot{\xi}}{|\dot{\xi}|}. \tag{46}$$

Once again this equation is similar to the one obtained by Miles [22] but with a different numerical factor in the plastic force term (his value is larger by a factor of 4). For $\dot{\xi} > 0$ Eq. (46) has the following solution with the initial condition $\dot{\xi}_0 = 0$:

$$\frac{\xi}{\xi_0} = A_0 + (1 - A_0)\cosh(\gamma t), \tag{47}$$

where $A_0 = \sqrt{2/3} Y/\rho_2 g \xi_0$ and $\gamma = \sqrt{kg}$.

Equations (46) and (47) show that instability requires $A_0 < 1$ or

$$\xi_0 > \sqrt{\frac{1}{3}} \frac{Y}{\rho_2 g}. \tag{48}$$

In the asymptotic regime we get

$$\frac{\xi_{(\infty)}(t)}{\xi_0} = \frac{1 - A_0}{2} e^{\gamma t}. \tag{49}$$

As far as we know no exact solutions or numerical simulations for this case of pure plastic behavior are available for comparison with the present results. Nevertheless, Dimonte *et al.* [47] reported that for a driving pressure of 10 GPa and a slab of thickness $H = \lambda/2$, numerical simulations, consistently with high explosives experiments of Ref. [18] (experiments suggest $0.30 < P_{cr} < 0.60$), predicted instability when the initial amplitude ξ_0 exceeds a critical value $\xi_{cr} = (2Y/\rho_2 g) P_{cr}$ with $P_{cr} \approx 0.4$. Previous analytical models (that assume $H \gg \lambda$) yield $P_{cr} \approx 1.15$ [22] and $P_{cr} \approx 1$ [33] while from the present model we get $P_{cr} \approx 0.3$. In spite of the good agreement of this value with the one reported by Dimonte *et al.* it should not be taken too literally since P_{cr} is expected to depend on the ratio H/λ [22–24,33].

IV. CONCLUDING REMARKS

We have presented an intuitively appealing approach to the RT instability with the aim of developing a tool for dealing with complex situations that occur in accelerated solid materials and that are difficult, or perhaps impossible, to treat with other analytical methods. It can be considered as a one-degree-of-freedom model but, different from previous models of this type based on an energy balance, the present one is based on a balance of forces. Although both approaches should be physically equivalent, our model allows for simple and rather accurate results. In fact, when the model is applied to the RT instability in fluids it produces the exact results for the classical situation including the effects of surface tension. When the model is applied to viscous fluids it is straightforward to find a formula well known as an excellent analytical approximation (error below 11%) [34,40–42].

In the case of perfectly elastic solids we have presented an approximate but rather accurate and general theory that includes the previous results obtained by means of mathematically rigorous methods but which are also so involved that it seems difficult to extend them to more realistic situations. The present model reproduces the asymptotic behavior of the perturbation growth for arbitrary Atwood numbers given in Ref. [21] and it also describes correctly the transient phase determined by the initial conditions [26]. This fact is very important because in practice the particular experimental conditions can determine different initial conditions. The RT unstable phase may also take place after a previous phase dominated by the RM instability and it will impose the initial conditions for the later RT phase. All these different initial conditions will also affect the asymptotic behavior. In fact, for the particular case of an initially stress-free solid we find that asymptotically the perturbation grows as if, initially, it would have had an amplitude $\xi_0/2(1 - k/k_c)$ which depends on the perturbation wave number as well as on the main parameters of the physical problem (ρ, g, G, ξ_0). A similar dependence is found for the oscillation amplitudes in the stable cases.

The model seems to be very suitable for dealing with more complex situations and we have considered, as in Ref. [21], not only solid/vacuum interfaces but also solid/viscous fluid interfaces. This is of great relevance to the experiments that are being designed at GSI Darmstadt within the framework of the application of the future FAIR project to the study of high energy density matter. An example of this is the LAPLAS experimental scheme shown in Fig. 1. In that case, simulations show that for the highest intensity that will be available in the new accelerator facility (around 10^{12} particles), for a thick shell of gold, the absorber region reaches a of pressure about 4 Mbar and it remains in liquid state during the whole implosion process. The pusher instead is driven by a maximum pressure of about 2.6 Mbar and it remains in solid state with temperatures below 2000 K during the acceleration phase. During the deceleration phase, the pusher starts to melt when the internal sample is strongly compressed. Thus solid/fluid interfaces will be present during all the experiment.

We have also applied our model to a perfectly rigid plastic solid and we have found results in agreement with reported data of simulations and experiments. However, it is well known that models for perfectly rigid plastic or perfectly

elastic solids cannot account for the variety and complexity of the phenomena observed in numerical simulations and experiments. As has been noticed by Terrones [21] a compelling theoretical treatment of RT instabilities in elastoplastic materials has yet to be developed. The model presented in this paper can serve as a guide for such a more complete theory which should be able to describe the transition from elastic to plastic behavior. Such a theory is a challenge that we expect can be met with the help of the method presented in this paper.

ACKNOWLEDGMENTS

The authors wish to thank M. Temporal and G. Wouchuk for very helpful discussions. One of us (A.R.P.) would like to thank the staff of the Heavy Ion Plasma Physics Group of the GSI Darmstadt for their very kind hospitality during his one-month stay in the Group. This work has been partially supported by the Ministerio de Ciencia y Tecnología (Grant No. FTN2003-00721) and by the Consejería de Ciencia y Tecnología of Spain, and by the BMBF of Germany.

[1] W. F. Henning, Nucl. Instrum. Methods Phys. Res. B **214**, 211 (2004).
[2] N. A. Tahir, A. Adonin, C. Deutsch, V. E. Fortov, N. Grandlouan, B. Geif, V. Gayaznov, D. H. H. Hoffmann, M. Kulish, I. V. Lomonosov, V. Mintsev, P. Ni, D. Nikolaev, A. R. Piriz, N. Shilkin, P. Spiller, A. Shutov, M. Temporal, V. Ternovoi, S. Udrea, and D. Varentsov, Nucl. Instrum. Methods Phys. Res. A **544**, 16 (2005).
[3] N. A. Tahir, D. H. H. Hoffmann, A. Kozyreva, A. Tauschwitz, A. Shutov, J. A. Maruhn, P. Spiller, U. Neuner, and R. Bock, Phys. Rev. E **63**, 016402 (2001).
[4] N. A. Tahir, H. Juranek, A. Shutov, R. Redmer, A. R. Piriz, M. Temporal, D. Varentsov, S. Udrea, D. H. H. Hoffmann, C. Deutsch, I. Lomonosov, and V. E. Fortov, Phys. Rev. B **67**, 184101 (2003).
[5] A. R. Piriz, R. F. Portugues, N. A. Tahir, and D. H. H. Hoffmann, Laser Part. Beams **20**, 427 (2002).
[6] N. A. Tahir, A. Kozyreva, D. H. H. Hoffmann, A. Shutov, P. Spiller, U. Neuner, A. Tauschwitz, J. Jacoby, M. Roth, J. A. Marhun, R. Bock, H. Juranek, and R. Redmer. Contrib. Plasma Phys. **41**, 609 (2001).
[7] M. Temporal, A. R. Piriz, N. Grandjouan, N. A. Tahir, and D. H. H. Hoffmann, Laser Part. Beams **21**, 427 (2003).
[8] A. R. Piriz, R. F. Portugues, N. A. Tahir, and D. H. H. Hoffmann, Phys. Rev. E **66**, 056403 (2002).
[9] E. Wigner and H. B. Huntington, J. Chem. Phys. **3**, 764 (1935).
[10] S. T. Weir, A. C. Mitchell, and W. J. Nellis, Phys. Rev. Lett. **76**, 1860 (1996).
[11] R. Arnold, E. Colton, S. Fenster, M. Foss, G. Magelssen, and A. Moretti, Nucl. Instrum. Methods Phys. Res. **199**, 557 (1982).
[12] A. R. Piriz, N. A. Tahir, D. H. H. Hoffmann, and M. Temporal, Phys. Rev. E **67**, 017501 (2003).
[13] A. R. Piriz, M. Temporal, J. J. Lopez-Cela, N. A. Tahir, and D. H. H. Hoffmann, Plasma Phys. Controlled Fusion **45**, 1733 (2003).
[14] R. K. Keinigs, W. L. Atchison, R. J. Faehl, V. A. Thomas, K. D. McLenithan, and R. J. Trainor, J. Appl. Phys. **85**, 7626 (1999).
[15] R. E. Reinovsky, W. E. Anderson, W. L. Atchison, C. E. Ekdahl, R. J. Faehl, I. R. Lindemuth, D. V. Morgan, M. Murillo, J. L. Stokes, and J. S. Shlachter, IEEE Trans. Plasma Sci. **30**, 1764 (2002).
[16] R. L. Bowers, J. M. Brownell, H. Lee, K. D. McLenithan, A. J. Scannapieco, and W. R. Shanhan, J. Appl. Phys. **83**, 4146 (1998).
[17] J. F. Barnes, P. J. Blewet, R. G. McQueen, K. A. Meyer, and D. Venable, J. Appl. Phys. **45**, 727 (1974).
[18] J. F. Barnes, D. H. Janney, R. K. London, K. A. Meyer, and D. H. Sharp, J. Appl. Phys. **51**, 4678 (1980).
[19] S. M. Bakharakh, O. B. Drennov, N. P. Kovalev, A. I. Lebedev, E. E. Meshkov, A. L. Mikhailov, N. V. Neumerzhitsky, P. N. Nizovtsev, V. A. Rayevsky, G. P. Simonov, V. P. Solovyev, and I. G. Zhidov, Lawrence Livermore National Laboratory Report No. UCRL-CR-126710, 1997 (unpublished).
[20] J. D. Colvin, M. Legrand, B. A. Remington, G. Shurtz, and S. V. Weber, J. Appl. Phys. **93**, 5287 (2003).
[21] G. Terrones, Phys. Rev. E **71**, 036306 (2005).
[22] J. W. Miles, General Dynamics Report No. GAMD-7335, AD 643161 (1966) (unpublished).
[23] G. N. White, Los Alamos National Laboratory Report No. LA-5225-MS (1973) (unpublished).
[24] A. C. Robinson and J. W. Swegle, J. Appl. Phys. **66**, 2859 (1989).
[25] J. K. Dienes, Phys. Fluids **21**, 736 (1978).
[26] B. J. Plohr and D. H. Sharp, ZAMP **49**, 786 (1998).
[27] J. G. Wouchuk, Phys. Rev. E **63**, 056303 (2001).
[28] J. G. Wouchuk, Phys. Plasmas **8**, 2890 (2001).
[29] J. W. Swegle and A. C. Robinson, J. Appl. Phys. **66**, 2838 (1989).
[30] E. L. Ruden and D. E. Bell, J. Appl. Phys. **82**, 163 (1997).
[31] E. Fermi, *The Collected Papers of Enrico Fermi*, edited by E. Amaldi *et al.* (University of Chicago Press, Chicago, 1962), Vol. 2, p. 813.
[32] G. I. Taylor, Proc. R. Soc. London, Ser. A **201**, 192 (1950).
[33] D. C. Drucker, *Mechanics Today*, edited by S. Nemat-Nasser (Pergamon, Oxford, 1980), Vol. 5, p. 37.
[34] S. Chandrasekhar, *Hydrodynamics and Hydromagnetic Stability* (Dover, New York, 1961).
[35] L. D. Landau and E. M. Lifshits, *Fluid Mechanics*, 2nd. ed. (Pergamon, Oxford, 1987).
[36] H. Poritsky, in *Proceedings of the First U.S. National Congress on Applied Mechanics*, edited by E. Sternberg (Am. Soc. Mech. Eng., New York, 1952), p. 813.
[37] T. G. Leighton, *The Acoustic Bubble* (Academic Press, London, 1997), p. 303.
[38] A. R. Piriz, J. Sanz, and L. F. Ibañez, Phys. Plasmas **4**, 1117 (1997).
[39] A. R. Piriz, Phys. Plasmas **8**, 997 (2001).

[40] R. Bellman and R. H. Pennington, Q. Appl. Math. **12**, 151 (1954).
[41] R. Hide, Proc. Cambridge Philos. Soc. **57**, 415 (1955).
[42] K. O. Mikaelian, Phys. Rev. E **47**, 375 (1993).
[43] K. O. Mikaelian, Phys. Rev. E **54**, 3676 (1996).
[44] R. Menikoff, R. C. Mjolsness, D. H. Sharp, and C. Zemach, Phys. Fluids **20**, 2000 (1977).
[45] J. W. Miles and J. K. Dienes, Phys. Fluids **9**, 2518 (1966).
[46] L. D. Landau and E. M. Lifshits, *Theory of Elasticity*, 3rd. ed. (Pergamon, Oxford, 1986).
[47] G. Dimonte, R. Gore, and M. Schneider, Phys. Rev. Lett. **80**, 1212 (1998).